

# The $\beta$ Subunit Increases the $\text{Ca}^{2+}$ Sensitivity of Large Conductance $\text{Ca}^{2+}$ -activated Potassium Channels by Retaining the Gating in the Bursting States

CRINA M. NIMIGEAN and KARL L. MAGLEBY

From the Department of Physiology and Biophysics, University of Miami School of Medicine, Miami, Florida 33101-6430

**ABSTRACT** Coexpression of the  $\beta$  subunit ( $\text{K}_{\text{V,Ca}}\beta$ ) with the  $\alpha$  subunit of mammalian large conductance  $\text{Ca}^{2+}$ -activated  $\text{K}^+$  (BK) channels greatly increases the apparent  $\text{Ca}^{2+}$  sensitivity of the channel. Using single-channel analysis to investigate the mechanism for this increase, we found that the  $\beta$  subunit increased open probability ( $P_o$ ) by increasing burst duration 20–100-fold, while having little effect on the durations of the gaps (closed intervals) between bursts or on the numbers of detected open and closed states entered during gating. The effect of the  $\beta$  subunit was not equivalent to raising intracellular  $\text{Ca}^{2+}$  in the absence of the beta subunit, suggesting that the  $\beta$  subunit does not act by increasing all the  $\text{Ca}^{2+}$  binding rates proportionally. The  $\beta$  subunit also inhibited transitions to subconductance levels. It is the retention of the BK channel in the bursting states by the  $\beta$  subunit that increases the apparent  $\text{Ca}^{2+}$  sensitivity of the channel. In the presence of the  $\beta$  subunit, each burst of openings is greatly amplified in duration through increases in both the numbers of openings per burst and in the mean open times. Native BK channels from cultured rat skeletal muscle were found to have bursting kinetics similar to channels expressed from alpha subunits alone.

**KEY WORDS:** large conductance  $\text{Ca}^{2+}$ -activated  $\text{K}^+$  channel • ion channel • subconductance • kinetics • accessory subunit

## INTRODUCTION

Large conductance  $\text{Ca}^{2+}$ -activated  $\text{K}^+$  channels (BK channels)<sup>1</sup> play an important role in regulating the excitability of nerve, muscle, and other cells by stabilizing the cell membrane at negative potentials (reviewed by Latorre et al., 1989; McManus, 1991; Kaczorowski et al., 1996). BK channels are activated by both intracellular calcium ( $\text{Ca}^{2+}_i$ ) and membrane depolarization, and hence can serve as an important link to couple the effects of  $\text{Ca}^{2+}_i$  and membrane potential, two common forms of signaling in cells. To facilitate this linkage, the  $\text{Ca}^{2+}_i$  sensitivity of BK channels, defined as the  $\text{Ca}^{2+}_i$  required for half-maximal activation at a given voltage, is set to match the specific needs of the various cells. In some tissues, such as smooth muscle, BK channels are highly  $\text{Ca}^{2+}_i$  sensitive, while in other tissues, such as skeletal muscle, the channels are much less  $\text{Ca}^{2+}$  sensitive (Singer and Walsh, 1987; McManus and Magleby, 1991; Tanaka et al., 1997).

Recent studies have given some insight into the molecular basis for differences in  $\text{Ca}^{2+}$  sensitivity. BK chan-

nels can be formed of either  $\alpha$  subunits alone or of  $\alpha$  together with  $\beta$  subunits (Adelman et al., 1992; Garcia-Calvo et al., 1994; McManus et al., 1995; Dworetzky et al., 1996; Tseng-Crank et al., 1996). The larger pore-forming  $\alpha$  subunits are encoded by the gene at the *slo* locus, mutations of which underlie the *Drosophila* *slowpoke* phenotype (Atkinson et al., 1991; Adelman et al., 1992; Butler et al., 1993; Pallanck and Ganetzky, 1994; Dworetzky et al., 1994; Tseng-Crank et al., 1994; Wallner et al., 1996). The  $\alpha$  (*slo*) subunit shows homology with the pore-forming subunits of the voltage-dependent superfamily of  $\text{K}^+$  channels, which have at least six putative transmembrane domains, a pore-forming region between S5 and S6, and an S4 voltage-sensor region (Atkinson et al., 1991; Salkoff et al., 1992; Butler et al., 1993; Jan and Jan, 1997). However, the  $\text{NH}_2$ - and  $\text{COOH}$ -terminal ends of the  $\alpha$  subunits differ from those of the superfamily. The  $\text{NH}_2$  terminus of mammalian  $\alpha$  subunits displays an additional transmembrane domain, S0, that places the amino terminal into the extracellular space and is required for the action of the  $\beta$  subunit (Wallner et al., 1996; Meera et al., 1997). The  $\text{COOH}$ -terminal tail is greatly extended, displays four hydrophobic domains, and appears to provide the  $\text{Ca}^{2+}$ -sensing domain of the channel (Wei et al., 1994; Schreiber and Salkoff, 1997). The  $\beta$  subunit, with two putative transmembrane domains, shows no homology with other ion channel subunits (Knaus et al., 1994).

Address correspondence to Karl L. Magleby, Ph.D., Department of Physiology and Biophysics, R430, P.O. Box 016430, Miami, FL 33101-6430. Fax: 305-243-6898; E-mail: kmagleby@mednet.med.miami.edu

<sup>1</sup>Abbreviations used in this paper: BK channel, large conductance  $\text{Ca}^{2+}$ -activated  $\text{K}^+$  channel; GFP, green fluorescent protein; HEK cells, human embryonic kidney cells.

While  $\alpha$  subunits assemble as tetramers to form functional channels by themselves (Shen et al., 1994),  $\beta$  subunits expressed alone do not (McManus et al., 1995). Rather,  $\beta$  subunits can associate with  $\alpha$  subunits in a 1:1 stoichiometry (Garcia-Calvo et al., 1994), increasing the apparent  $\text{Ca}^{2+}$  sensitivity of the  $\alpha$  subunits  $\sim 10$ -fold (McManus et al., 1995). It is the presence of the  $\beta$  subunit that confers the greatly increased  $\text{Ca}^{2+}$  sensitivity to BK channels in smooth muscle (McManus et al., 1995; Tanaka et al., 1997). Although it is known that the  $\beta$  subunit slows activation and deactivation kinetics (Dworetzky et al., 1996; Meera et al., 1996; Tseng-Crank et al., 1996), while having little effect on channel open probability in the absence of  $\text{Ca}^{2+}$ ; (Meera et al., 1996), the mechanism by which the  $\beta$  subunit increases the apparent  $\text{Ca}^{2+}$  sensitivity of BK channels is not known. The  $\beta$  subunit could increase apparent  $\text{Ca}^{2+}$  sensitivity through fundamental changes in the gating mechanism, such as by generating additional conformational states or  $\text{Ca}^{2+}$ -binding sites. Alternatively, the  $\beta$  subunit might act by modulating the gating of the  $\alpha$  subunit to increase the rate of  $\text{Ca}^{2+}$  binding or to change the rates of selected transitions among the various conformational states.

We now use the resolving power of the single-channel recording technique to differentiate among these possible types of action by studying the kinetics of single BK channels comprised of  $\alpha$  subunits alone, or of both  $\alpha$  and  $\beta$  subunits. Our data suggest that the  $\beta$  subunit does not act by changing the fundamental gating mechanism, as neither the Hill coefficients for  $\text{Ca}^{2+}$  binding nor the numbers of detected kinetic states entered during gating were changed by the  $\beta$  subunit. The data also suggest that the  $\beta$  subunit had little effect on the initial  $\text{Ca}^{2+}$ -binding steps involved in activation of the channel, as the durations of the gaps (the long closed intervals) between bursts of activity were little changed. Instead, the  $\beta$  subunit increased  $\text{Ca}^{2+}$  sensitivity through selected modulation of transition rates to retain the channel in the open and closed states that generate the bursts of activity (bursting states), increasing burst duration 20–100-fold. We also found that the  $\beta$  subunit inhibited transitions to subconductance states, and that the gating of native BK channels from cultured rat skeletal muscle was similar to the gating of BK channels expressed from  $\alpha$  subunits alone.

## METHODS

### *Heterologous Expression of BK Channels in Human Embryonic Kidney 293 Cells*

Human embryonic kidney (HEK) 293 cells were transiently transfected with expression vectors (pcDNA3) encoding the  $\alpha$  subunit (*mslo* from mouse, Genbank accession number MMU09383) and the  $\beta$  subunit (bovine  $\beta$ , Genbank accession number L26101) of

BK channels, kindly provided by Merck Research Laboratories, and also with an expression vector encoding the green fluorescent protein (GFP, Plasmid pGreen Lantern-1; GIBCO BRL). Cells were transfected transiently using the Lipofectamine Reagent (Life Technologies, Inc.). The GFP was used to monitor successfully transfected cells. For transfection, cells at 30–40% confluency in 30 mm recording Falcon dishes were incubated with a mixture of the plasmids (total of 1  $\mu\text{g}$  DNA), Lipofectamine Reagent (optimal results at 7  $\mu\text{l}$ ), and Opti-MEM I Reduced Serum Medium (GIBCO BRL). The mixture was left on the cells for 1 h, after which it was replaced with standard tissue culture media: DMEM with 5% fetal bovine serum (GIBCO BRL) and 1% penicillin-streptomycin solution (Sigma Chemical Co.). The cells were patch-clamped 2–3 d after transfection.

In the coexpression experiments, a fourfold molar excess of plasmid encoding the  $\beta$  subunit was used to drive coassembly with the  $\alpha$  subunits in the expressed channels (McManus et al., 1995). Using the same promoter (cytomegalovirus) for the  $\alpha$  and  $\beta$  subunits and the GFP increased the probability that if the GFP was expressed, the included subunits would also be expressed. While we did not prove directly that all BK channels studied from cells cotransfected with plasmids encoding for  $\alpha$  and  $\beta$  subunits were indeed composed of both  $\alpha$  and  $\beta$  subunits, the markedly different bursting kinetics of BK channels from such cells (see RESULTS) indicated that the coexpression of the  $\beta$  with the  $\alpha$  subunit altered the gating of the channels.

### *Solutions*

The intracellular solution contained 175 mM KCl, 5 mM TES [*N*-tris(hydroxymethyl)methyl-2-aminoethane sulfonic acid] pH buffer, and 10 mM EGTA and 10 mM HEDTA to buffer the  $\text{Ca}^{2+}$  (see below). The extracellular solution contained either 150 or 175 mM KCl and 5 mM TES and had no added  $\text{Ca}^{2+}$  or  $\text{Ca}^{2+}$  buffers. Both the intracellular and extracellular solutions were brought to pH 7. The amount of  $\text{Ca}^{2+}$  added to the intracellular solution to obtain approximate free  $\text{Ca}^{2+}$  concentrations of 0.1–100  $\mu\text{M}$  was calculated using stability constants for EGTA from Smith and Miller (1985) and for HEDTA from Martell and Smith (1993). These solutions were then calibrated using a  $\text{Ca}^{2+}$  electrode (Ionplus from Orion Research, Inc.) standardized against solutions with KCl and TES (as in the experimental solutions) in which a known amount of  $\text{Ca}^{2+}$  was added. Before adding  $\text{Ca}^{2+}$ , any contaminating divalent cations were removed from the solution by treatment with Chelex 100 (Bio-Rad Laboratories). The solutions bathing the intracellular side of the patch were changed by means of a valve-controlled, gravity-fed perfusion system using a microchamber (Barrett et al., 1982).

### *Single-Channel Recording and Analysis*

Currents flowing through single BK channels in patches of surface membrane excised from HEK 293 cells transfected with clones for either  $\alpha$  or  $\alpha$  and  $\beta$  subunits were recorded using the patch-clamp technique (Hamill et al., 1981). All recordings were made using the excised inside-out configuration in which the intracellular surface of the patch was exposed to the bathing solution. BK channels were identified by their large conductance and characteristic voltage and  $\text{Ca}^{2+}$  dependence (Barrett et al., 1982). Endogenous BK channels in nontransfected HEK 293 cells were not seen, but we cannot exclude that they might exist at a low density. Currents were recorded with an Axopatch 200A amplifier (Axon Instruments) and stored on VCR tapes using a VR-10B digital data recorder. The currents were then analyzed using custom programs written in the laboratory. Single-channel

patches were identified by observing openings to only a single open-channel conductance level during several minutes of recording in which the open probability was  $>0.4$ . Except for two experiments in which patches containing two BK channels were used to measure the effect of  $\text{Ca}^{2+}$  on open probability ( $P_o$ ), all data were from patches containing a single BK channel. Experiments were performed at room temperature (20–25°C).

Single-channel current records were low-pass filtered with a four-pole Bessel filter to give a final effective filtering of typically 4.5–10 kHz (–3 dB) and were sampled by computer at a rate of 125–250 kHz. The methods used to select the level of filtering to exclude false events that could arise from noise, measure interval durations with half-amplitude threshold analysis, and use stability plots to test for stability and identify activity in different modes have been described previously, including the precautions taken to prevent artifacts in the analysis (McManus et al., 1987; McManus and Magleby, 1988, 1989; Magleby, 1992). The kinetic analysis in this study was restricted to channel activity in the normal mode, which typically involves  $\sim 96\%$  of the detected intervals (McManus and Magleby, 1988). Activity in modes other than normal, including the low activity mode (Rothberg et al., 1996), was removed before analysis, as were transitions to subconductance levels, except when the subconductance levels were being studied specifically. The numbers of intervals during normal activity analyzed for each experimental condition ranged from  $\sim 1,500$  to  $\sim 200,000$ , with the greater numbers of intervals being obtained for higher  $\text{Ca}^{2+}_i$  where the channel activity was higher.

The methods used to log-bin the intervals into dwell-time distributions, fit the distributions with sums of exponentials using maximum likelihood fitting techniques (intervals less than two dead times were excluded from the fitting), and determine the number of significant exponential components with the likelihood ratio test have been described previously (McManus and Magleby, 1988, 1991; Colquhoun and Sigworth, 1995). Dwell-time distributions are plotted with the Sigworth and Sine (1987) transformation, which plots the square root of the number of intervals per bin without correcting for the logarithmic increase in bin width with time. With this transform, the peaks in the plots fall at the time constants of the major exponential components.

The method of defining a critical gap (closed interval) in order to identify bursts is detailed in Magleby and Pallotta (1983). In brief, the distributions of closed-interval durations were first fitted with, typically, the sum of five exponential components. The closed intervals from the one to two exponential components with the longest time constants were then defined as gaps between bursts, as there was typically a difference of one to three orders of magnitude in the time constants separating the components generating gaps between bursts from those generating closed intervals within bursts. A critical time was then defined to separate closed intervals that were gaps between bursts from those that were gaps within bursts, so that the numbers of misclassified closed intervals would cancel out. The critical time was found to be relatively insensitive to the numbers of exponentials used to fit the dwell-time distribution. Burst analysis was performed on data sets from single channels in which  $P_o$  was typically less than  $\sim 0.8$ , since it became increasingly difficult to define gaps between bursts as the  $P_o$  approached its maximum value of  $\sim 0.96$  during activity in the normal mode.

#### *Native BK Channels from Cultured Rat Skeletal Muscle*

The parameters describing bursting kinetics for native BK channels from cultured rat skeletal muscle were obtained by analyzing data from previous experiments by McManus and Magleby (1991) and Rothberg and Magleby (1998), which can be consulted for the experimental details.

## RESULTS

### *The $\beta$ Subunit Alters the Gating of *mslo* as Revealed by Single-Channel Kinetics*

The patch-clamp technique was used to record currents from single BK channels in patches of membrane excised from HEK 293 cells after transfection with either the  $\alpha$  subunit (referred to as  $\alpha$  channels) or with both  $\alpha$  and  $\beta$  subunits (referred to as  $\alpha + \beta$  channels). The effects of the  $\beta$  subunit on the gating are illustrated in Fig. 1, which shows representative single-channel currents recorded with 1.8, 3.6, or 5.4  $\mu\text{M}$  calcium at the inner membrane surface ( $\text{Ca}^{2+}_i$ ). The activity of both  $\alpha$  and  $\alpha + \beta$  channels increased with increasing  $\text{Ca}^{2+}_i$ , and for each  $\text{Ca}^{2+}_i$ , the presence of the  $\beta$  subunit further increased the activity. These observations are fully consistent with earlier studies, using mainly currents through multiple channels, that established that the  $\beta$  subunit increases the open probability ( $P_o$ ) (McManus et al., 1995; Dworetzky et al., 1996; Meera et al., 1996; Tseng-Crank et al., 1996).

The first clues towards the mechanism by which the  $\beta$  subunit increases  $P_o$  are readily apparent in Fig. 1. The  $\beta$  subunit had marked effects on the single-channel gating kinetics: at a fixed  $\text{Ca}^{2+}_i$ , the  $\beta$  subunit greatly increased the durations of the bursts of activity while appearing to have little effect on the durations of the gaps (closed intervals) between bursts. This characteristic effect of the  $\beta$  subunit on the bursting kinetics of the single-channel current records was consistently observed in comparisons of data from 19  $\alpha$  channels and 10  $\alpha + \beta$  channels. 10 of these channels (5  $\alpha$  and 5  $\alpha + \beta$ ) were then analyzed in detail to obtain the results in the rest of the paper.

### *The $\beta$ Subunit Increases $P_o$ while Having Little Effect on the Hill Coefficient*

As evident in Fig. 1,  $\alpha + \beta$  channels are open a greater fraction of the time at a given  $\text{Ca}^{2+}_i$  than are  $\alpha$  channels. To further examine this difference in  $\text{Ca}^{2+}$  sensitivity, we plotted  $P_o$  vs.  $\text{Ca}^{2+}_i$  for  $\alpha$  and for  $\alpha + \beta$  channels. Typical results are shown in Fig. 2 A, where the  $\text{Ca}^{2+}_i$  for a  $P_o$  of 0.5 ( $K_d$ ) was  $9.2 \pm 2.3 \mu\text{M}$  (mean  $\pm$  SD) for the  $\alpha$  channels, shifting to  $2.6 \pm 0.52 \mu\text{M}$  for the  $\alpha + \beta$  channels (+30 mV). In a series of similar experiments, the  $K_d$  was  $14.2 \pm 7.2 \mu\text{M}$  (range: 6.9–22.86  $\mu\text{M}$ ,  $n = 5$ ) for  $\alpha$  channels and  $3.5 \pm 1.3 \mu\text{M}$  (range: 2.2–4.9  $\mu\text{M}$ ,  $n = 5$ ) for  $\alpha + \beta$  channels. Thus, the effect of the  $\beta$  subunit on  $P_o$  was equivalent to increasing  $\text{Ca}^{2+}_i$  approximately fourfold.

The Hill coefficients derived from the  $P_o$  vs.  $\text{Ca}^{2+}_i$  plots like those in Fig. 2 A were  $4.6 \pm 1.8$  for  $\alpha$  channels and  $4.5 \pm 1.6$  (mean  $\pm$  SD) for  $\alpha + \beta$  channels (the slopes were not significantly different:  $P > 0.9$ ), suggesting that four to five  $\text{Ca}^{2+}$  ions (range: 2–6) typically

bound to activate the BK channels in our experiments. These values are within the ranges of 2–5 typically observed for both native and cloned BK channels (McManus, 1991; Cox et al., 1997, and references therein).

*The  $\beta$  Subunit Increases Mean Open Time and Decreases Mean Closed Time*

To investigate the basis for the  $\beta$  subunit-induced increase in  $P_o$ , we measured the observed durations of the open and closed intervals for data obtained from patches containing either a single  $\alpha$  or an  $\alpha + \beta$  channel over a range of  $Ca^{2+}_i$ . Since determinations of observed mean open- and closed-interval duration are highly dependent on the time resolution, comparisons between specific  $\alpha$  and  $\alpha + \beta$  channels were made only for data obtained at the same level of filtering. Results are shown in Fig. 2, B and C, for a representative comparison, where the  $\beta$  subunit increased mean open times 3–7-fold and decreased mean closed times  $\sim 10$ -fold over the examined ranges of  $Ca^{2+}_i$ . Similar results were found for comparisons between four additional  $\alpha$  and four additional  $\alpha + \beta$  channels, each channel from a different experiment, paired for the same level of filtering, over a range of filtering (4.5–10 KHz).

Thus, the  $\beta$  subunit increases  $P_o$  through a dual effect of increasing observed mean open times and decreasing observed mean closed times. (It will be shown in a later section that the decrease in mean closed times with the  $\beta$  subunit results in large part from a decrease in the frequency, rather than the duration, of the longer closed intervals.) At high levels of  $Ca^{2+}_i$ , and consequently high  $P_o$ , the mean durations of the closed intervals were brief, and the  $\beta$  subunit had less of an effect on the durations of these already brief closed intervals. We did not explore the effects of nominally zero  $Ca^{2+}_i$ , where the  $\beta$  subunit has been reported to have little effect on  $P_o$  (Meera et al., 1996).

*The  $\beta$  Subunit Does Not Change the Number of Detected Kinetic States Entered during Gating*

The gating of BK channels has been described by kinetic schemes in which the channel makes transformations among a number of different kinetic states (e.g., McManus and Magleby, 1991; Wu et al., 1995; Cox et al., 1997). To examine whether the  $\beta$  subunit changes the number of kinetic states entered during gating, we fitted sums of exponential components to dwell-time distributions (frequency histograms) of open and closed

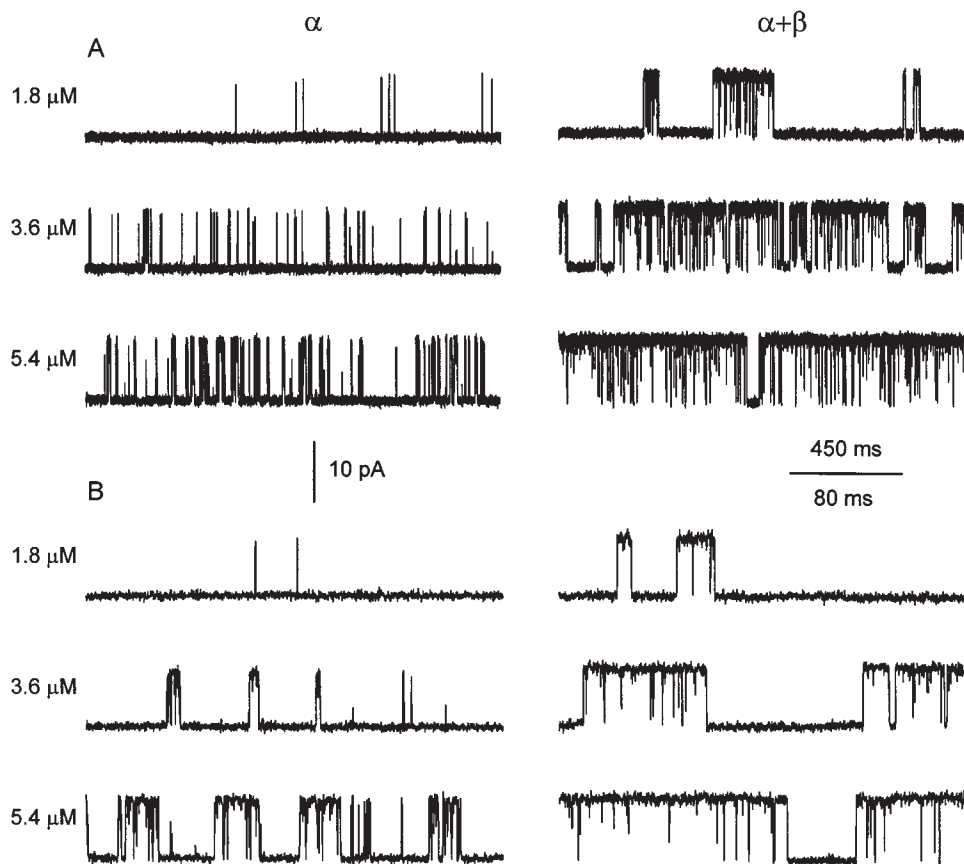


FIGURE 1. Single-channel current traces recorded from BK channels expressed from  $\alpha$  or  $\alpha + \beta$  subunits. Representative currents recorded with the patch-clamp technique from inside-out patches of membrane excised from HEK 293 cells transfected with only  $\alpha$  subunits ( $\alpha$ ) or with both  $\alpha$  and  $\beta$  subunits ( $\alpha + \beta$ ) with 1.8, 3.6, or 5.4  $\mu M$   $Ca^{2+}_i$ ; and with a membrane potential of +30 mV. Data are presented on slow (A) and fast (B) time bases. The average  $P_o$  for the entire record from which each excerpt was obtained were: 0.0041, 0.087, and 0.16 for the  $\alpha$  channel (top to bottom), and 0.15, 0.86, and 0.95 for the  $\alpha + \beta$  channel. The  $\beta$  subunit increased burst duration and  $P_o$ . Current traces were low-pass filtered at 2 kHz for display. Effective filtering was 9 kHz for analysis. Symmetrical 175 mM KCl (see METHODS).  $\alpha$  Channel, C62;  $\alpha + \beta$  channel, C64.

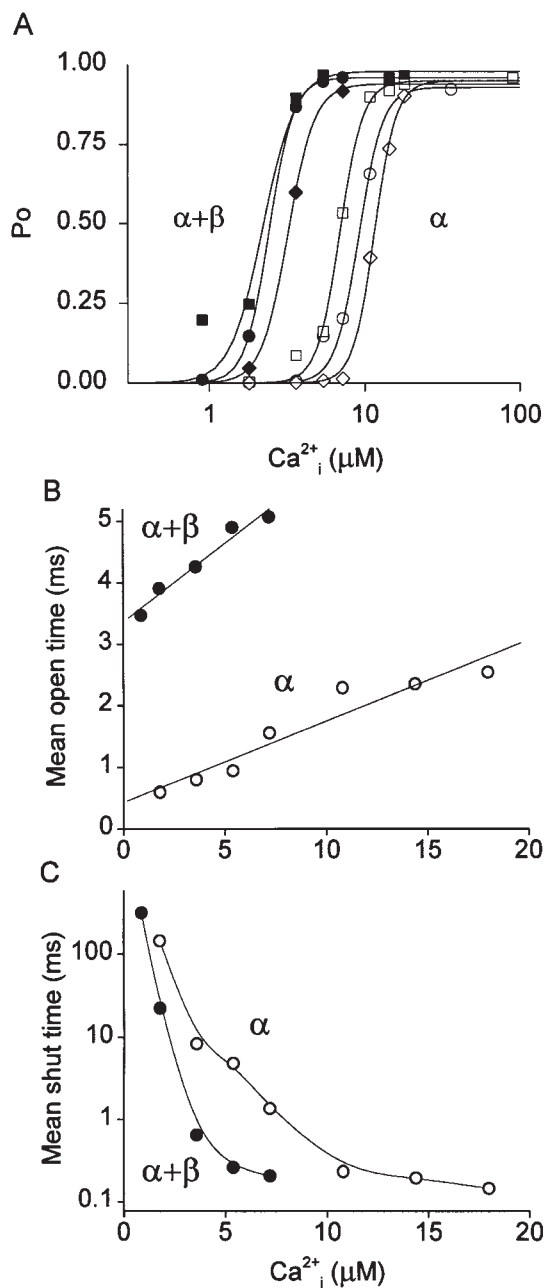


FIGURE 2. The  $\beta$  subunit increases  $P_o$  by increasing mean open times and decreasing mean closed times over a range of  $Ca^{2+}_i$ . (A) Plots of  $P_o$  vs.  $Ca^{2+}_i$  for  $\alpha$  channels (open symbols) and  $\alpha + \beta$  channels (filled symbols). Four of the six examined patches contained a single BK channel and two contained two BK channels. Each symbol type plots data from a different patch. The lines are fits of each symbol to the Hill equation, with the mean values of the parameters given in the text. Membrane potential, +30 mV. (B and C) Plots of mean open and closed times vs.  $Ca^{2+}_i$  for one representative  $\alpha$  channel (open symbols) and one representative  $\alpha + \beta$  channel (filled symbols). The straight lines (linear least square fits to the logs of the values) and curved lines (B-spline) are used to group the points for viewing in this and the following figures, unless indicated otherwise. (B and C) Same experimental conditions and channels as used for Fig. 1

interval durations for four single  $\alpha$  and three single  $\alpha + \beta$  channels. The numbers of significant exponential components required to fit the distributions gives an estimate of the minimum number of states entered during gating (Colquhoun and Hawkes, 1981, 1995). (Examples of dwell-time distributions will be presented in a later section.)

Fig. 3 plots the number of significant exponential components required to describe the open (A) and closed (B) dwell-time distributions for  $\alpha$  channels and  $\alpha + \beta$  channels. The estimates are plotted against the numbers of analyzed intervals, as the ability to detect exponential components is dependent on the numbers of intervals analyzed (McManus and Magleby, 1988). Estimates of the minimal numbers of open states (the number of significant exponential components) ranged from two to four for both types of channels, with the lower estimates of two open states associated with the smaller data sets. The mean number of detected open states for  $\alpha$  channels ( $3.0 \pm 0.5$ ; mean  $\pm$  SD) was not significantly different ( $P > 0.38$ , Mann-Whitney test, from Snedecor and Cochran, 1989) from the mean number of detected open states for  $\alpha + \beta$  channels ( $3.1 \pm 0.6$ ). Estimates of the numbers of detected closed states ranged from three to seven for  $\alpha$  channels and from four to seven for  $\alpha + \beta$  channels, with the estimate of three associated with a small data set. The mean number of detected closed states for  $\alpha$  channels ( $5.4 \pm 0.9$ ) was not significantly different ( $P > 0.37$ , Mann-Whitney test) from the mean number of detected closed states for  $\alpha + \beta$  channels ( $5.6 \pm 1.0$ ).

While it cannot be ruled out that changes in the numbers of kinetic states did occur with the  $\beta$  subunit but were not detected due to overlapping time constants and/or small areas of some of the exponential components, the data in Fig. 3 do indicate that the pronounced effect of the  $\beta$  subunit on channel activity did not arise from an obvious change in the numbers of detected kinetic states entered during gating. This observation, that the  $\beta$  subunit did not change the numbers of detected kinetic states, and the observation in a previous section that the  $\beta$  subunit did not change the Hill coefficients, suggests that the  $\beta$  subunit may exert its effects by changing transition rates among states rather than through fundamental changes in the gating mechanism, such as changes in the numbers of states or in the number of  $Ca^{2+}$ -binding sites.

#### The $\beta$ Subunit Greatly Increases Burst Duration

As a first step towards determining which transition rates may be affected, we examined the effect of the  $\beta$  subunit on bursting kinetics, since the single-channel records in Fig. 1 suggest that the  $\beta$  subunit greatly increases the durations of the bursts. A critical gap (closed interval between bursts of openings) was used

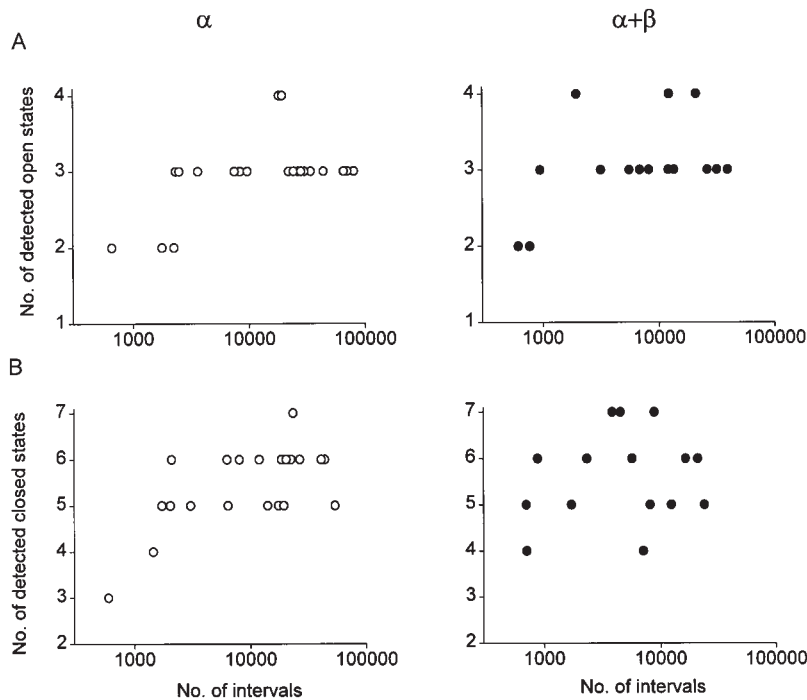


FIGURE 3. The  $\beta$  subunit does not change the number of detected open and closed states entered during gating. Estimates of the minimum number of detected open (A) and closed (B) states entered during gating are plotted against the number of intervals analyzed. The  $\beta$  subunit had no significant effect on the number of open ( $P > 0.58$ ) or closed ( $P > 0.53$ ) states. Estimates for  $\alpha$  channels are from fitting 21 sets of data from four channels, and those for  $\alpha + \beta$  channels are from 15 sets of data from three channels. The numbers of fitted intervals ranged from  $\sim 600$  to  $\sim 85,000$ . Data were obtained over a range of  $Ca^{2+}_i$  for both types of channels. There was no obvious effect of  $Ca^{2+}_i$  on the estimated numbers of states, so the estimates obtained at different  $Ca^{2+}_i$  are plotted on the same graph.

to identify bursts (see METHODS). Over the examined range of  $Ca^{2+}_i$ , the  $\beta$  subunit increased mean burst duration 20–100-fold (Fig. 4 A), while having little effect on the mean durations of the gaps (closed intervals) between or within bursts (Fig. 4 B).

This marked increase in mean burst duration by the  $\beta$  subunit was associated with pronounced increases in both the mean open times (Fig. 2 B) and in the mean number of openings per burst (Fig. 4 C). Since the addition of each opening to a burst requires an intervening (brief) closed interval, the numbers of closings per burst (given by one less than the number of openings in Fig. 4 C) also increased dramatically. The  $\beta$  subunit-induced lengthening of bursts decreased the fraction of the total closed intervals that were gaps between bursts (Fig. 4 D). For example, with  $3.6 \mu M Ca^{2+}_i$ , 21.7% of the observed closed intervals were gaps between bursts for  $\alpha$  channels, and this decreased to 1.8% for  $\alpha + \beta$  channels. Since the gaps between bursts are the longer closed intervals, this fractional reduction in the numbers of such intervals by the  $\beta$  subunit contributes greatly towards the increase in  $P_o$  by the  $\beta$  subunit.

Since estimates of both mean burst duration and the mean duration of gaps between bursts were relatively insensitive to the level of filtering, these parameters were compared directly for five  $\alpha$  channels and five  $\alpha + \beta$  channels, each obtained from a patch containing a single channel, in Fig. 4, E and F. The data from the 10 channels support the representative data shown in Fig. 4, A and B, for one channel of each type: the  $\beta$  subunit greatly increased mean burst duration while having lit-

tle effect on the duration of gaps between bursts. While there was considerable variability in estimates of mean burst duration among channels of the same type, all of the individual estimates of mean burst duration for  $\alpha$  channels when compared with  $\alpha + \beta$  channels were clearly separated at each examined  $Ca^{2+}_i$ , differing by at least an order of magnitude (Fig. 4 E). Hence, the magnitude of the effect of the  $\beta$  subunit on mean burst duration was greater than the variability among channels of the same type.

Since the mean open time, the mean number of openings per burst, and the mean duration of the gaps within bursts were all highly sensitive to differences in filtering, we only compared estimates of these parameters for channels that were filtered the same. Results similar to those in Figs. 2, B and C, and 4, A–D, were found for four such additional detailed comparisons between  $\alpha$  and  $\alpha + \beta$  channels, paired for the same level of filtering. In each case, the  $\beta$  subunit increased  $P_o$  by prolonging the bursts through increases in both the numbers of openings per burst and in the mean open time. Prolonging the bursts also decreased the fraction of shut intervals that were gaps between bursts by preventing the channel from entering the longer closed intervals that separate bursts.

#### *Increasing $P_o$ with the $\beta$ Subunit Was Not Equivalent to Increasing $Ca^{2+}_i$*

Similar to the effects of the  $\beta$  subunit on increasing mean open time, increasing  $Ca^{2+}_i$  also increases mean

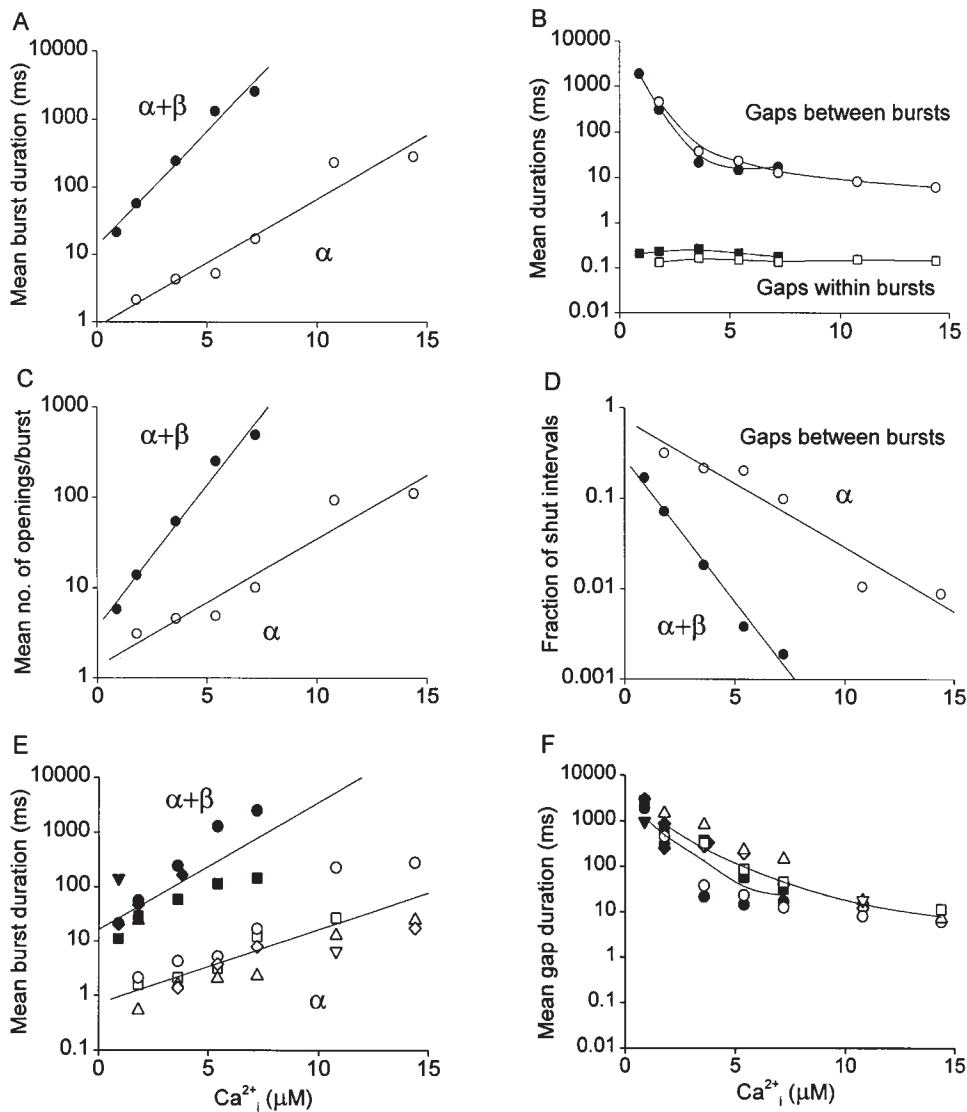


FIGURE 4. Differences in bursting kinetics between  $\alpha$  and  $\alpha + \beta$  channels. Bursts of intervals were identified with a critical gap (closed interval duration), as defined in METHODS. Each burst included all open and closed intervals between two closed intervals with durations greater than the critical gap. Over the examined range of  $\text{Ca}^{2+}_i$ , the  $\beta$  subunit greatly increased mean burst duration (A) and the mean number of openings per burst (C), while having little effect on the mean durations of the gaps (closed interval durations) between or within bursts (B), and decreasing the fraction of total closed intervals that represent gaps between bursts (D). Data are plotted for a single representative  $\alpha$  channel and a single representative  $\alpha + \beta$  channel. Same experimental conditions and channels as used for Fig. 1. (E and F) The mean burst duration and mean duration of gaps between bursts are plotted for five patches, each containing a single  $\alpha$  channel (open symbols), and another five patches, each containing a single  $\alpha + \beta$  channel (filled symbols). Each symbol type plots data from a different channel. The continuous lines in F are B-spline lines passing through the means of the logs of mean gap duration at each  $\text{Ca}^{2+}_i$  for the  $\alpha$  (top line) and  $\alpha + \beta$  (bottom line) channels.

open times for BK channels (Fig. 2 B; McManus and Magleby, 1991) and the numbers of openings per burst (Fig. 4 C; Magleby and Pallotta, 1983). Thus, a potential mechanism for the action of the  $\beta$  subunit is that it may increase the rates at which the channel binds the activating  $\text{Ca}^{2+}$  ions. If the addition of the  $\beta$  subunit increases all the  $\text{Ca}^{2+}$ -binding rates proportionally, then  $\alpha$  and  $\alpha + \beta$  channels should display identical kinetics when the  $\text{Ca}^{2+}_i$  is adjusted to give the same  $P_o$  for both types of channels. To examine this possibility, we compared the dwell-time distributions of  $\alpha$  and  $\alpha + \beta$  channels at the same  $P_o$ .

Results are shown in Fig. 5, which presents open dwell-time distributions on the left and closed dwell-time distributions on the right for both  $\alpha$  and  $\alpha + \beta$  channels, each at two different  $\text{Ca}^{2+}_i$ . At  $1.8 \mu\text{M} \text{Ca}^{2+}_i$ , the  $P_o$  for the  $\alpha$  channel was 0.004 (Fig. 5 A), while the  $P_o$  for the  $\alpha + \beta$  channel was 0.15 (Fig. 5 B). The increase in  $P_o$  induced by the  $\beta$  subunit was due to both a

pronounced shift in the open intervals to longer durations and a marked decrease in the number of longer closed intervals (gaps between bursts), as indicated by a decrease in the amplitude of the component marked gaps.

By increasing  $\text{Ca}^{2+}_i$  from  $1.8$  to  $5.4 \mu\text{M}$ , the  $P_o$  of the  $\alpha$  channel was increased from 0.004 to 0.16 (Fig. 5 C) to approximate the  $P_o$  of 0.15 for the  $\alpha + \beta$  channel at  $1.8 \mu\text{M} \text{Ca}^{2+}_i$  (Fig. 5 B). A comparison of the dwell-time distributions for the  $\alpha$  and  $\alpha + \beta$  channels at the same  $P_o$  showed marked differences in the kinetics: both the mean open times and the mean durations of the gaps between bursts were approximately an order of magnitude less for the  $\alpha$  channel (Fig. 5 C) than for the  $\alpha + \beta$  channel (Fig. 5 B), while the relative numbers of gaps between bursts were greater for the  $\alpha$  channel than for the  $\alpha + \beta$  channel. These marked differences in the kinetics of  $\alpha$  and  $\alpha + \beta$  channels at the same  $P_o$  exclude the possibility that the  $\beta$  subunit acts by the same pro-

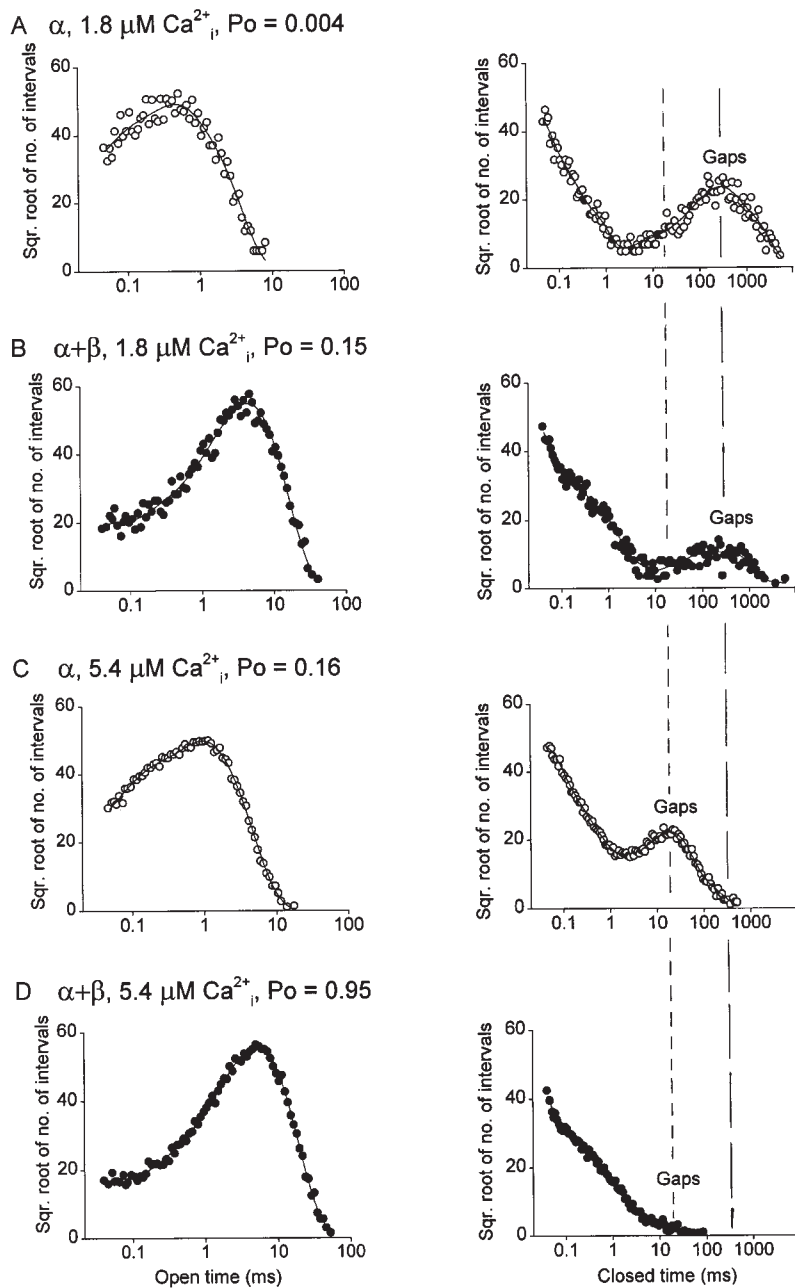


FIGURE 5. Dwell-time distributions obtained at the same  $P_o$  for  $\alpha$  channels and for  $\alpha + \beta$  channels indicate that the  $\beta$  subunit increases  $P_o$  differently than  $\text{Ca}^{2+}_i$ . The open and closed interval durations were log-binned and the square root of the number of intervals in each bin was plotted against the bin midtimes (see METHODS) for one  $\alpha$  channel and one  $\alpha + \beta$  channel at both 1.8 and 5.4  $\mu\text{M}$   $\text{Ca}^{2+}_i$ , as indicated. Compare A with C to see the effect of increasing  $\text{Ca}^{2+}_i$  on  $\alpha$  channels and B with D to see the effect of increasing  $\text{Ca}^{2+}_i$  on  $\alpha + \beta$  channels. Compare B with C to see the differences in distributions between  $\alpha$  and  $\alpha + \beta$  channels at the same  $P_o$ . Compare A with B to see the differences in the distributions between  $\alpha$  and  $\alpha + \beta$  channels at 1.8  $\mu\text{M}$   $\text{Ca}^{2+}_i$ , and C with D to see the differences in the distributions between  $\alpha$  and  $\alpha + \beta$  channels at 5.4  $\mu\text{M}$   $\text{Ca}^{2+}_i$ . To allow direct comparisons of the distributions, the number of intervals was normalized to 100,000 in each case. The mean durations of the gaps between bursts are indicated by the lines with long dashes for 1.8  $\mu\text{M}$   $\text{Ca}^{2+}_i$  and the lines with short dashes for 5.4  $\mu\text{M}$   $\text{Ca}^{2+}_i$ . The continuous lines are fits with sums of exponential components with time constants (ms) and areas of: (A, open) 0.066, 0.18; 0.32, 0.40; 0.98, 0.42. (A, closed) 0.023, 0.51; 0.090, 0.22; 0.40, 0.074; 200, 0.12; 850, 0.079. (B, open) 0.031, 0.065; 0.19, 0.058; 4.30, 0.88. (B, closed) 0.023, 0.59; 0.15, 0.24; 0.77, 0.12; 85, 0.022; 490, 0.026. (C, open) 0.12, 0.22; 0.64, 0.30; 1.4, 0.49. (C, closed) 0.038, 0.54; 0.17, 0.23; 0.85, 0.061; 17.5, 0.14; 65, 0.020. (D, open) 0.032, 0.050; 0.21, 0.037; 5.2, 0.92. (D, closed) 0.018, 0.63; 0.10, 0.24; 0.50, 0.12; 2.13, 0.014; 13, 0.0021. Same experimental conditions and channels as used for Fig. 1.

portional increases in all the rate constants for  $\text{Ca}^{2+}$  binding.

#### The $\beta$ Subunit Has Little Effect on the Durations of the Gaps between Bursts

One reason why increasing  $P_o$  with the  $\beta$  subunit was not equivalent to increasing  $\text{Ca}^{2+}_i$  in the absence of the  $\beta$  subunit was the differential effects of the  $\beta$  subunit and  $\text{Ca}^{2+}_i$  on the gaps between bursts. Fig. 4, B and D, shows that the  $\beta$  subunit had little effect on the durations of the gaps between bursts, while decreasing their relative numbers. This can also be seen in Fig. 5, where the addition of the  $\beta$  subunit at a fixed  $\text{Ca}^{2+}_i$  had little

effect on the mean durations of the gaps between bursts (positions of the peaks labeled gaps) while it decreased the relative numbers of the gaps, as indicated by the decrease in amplitude of the peaks in the presence of the  $\beta$  subunit (compare Fig. 5 A to B for 1.8  $\mu\text{M}$   $\text{Ca}^{2+}_i$  and Fig. 5 C to D for 5.4  $\mu\text{M}$   $\text{Ca}^{2+}_i$ ).

#### $\text{Ca}^{2+}_i$ Decreases the Durations of the Gaps between Bursts

In contrast to the little effect of the  $\beta$  subunit on the durations of the gaps between bursts, increasing  $P_o$  by raising  $\text{Ca}^{2+}_i$  decreased the durations of gaps between bursts for both  $\alpha$  and  $\alpha + \beta$  channels. This decrease is shown in Fig. 4 B, where increasing  $\text{Ca}^{2+}_i$  reduced the



durations of gaps between bursts for both types of channels. This effect of  $\text{Ca}^{2+}_i$  in reducing the durations of gaps between bursts for both the  $\alpha$  and  $\alpha + \beta$  channels can also be seen in the dwell-time distributions in Fig. 5, where increasing  $\text{Ca}^{2+}_i$  from 1.8 to 5.4  $\mu\text{M}$  shifted the peaks labeled gaps to briefer durations (compare Fig. 5 A to C for  $\alpha$  channels and Fig. 5 B to D for  $\alpha + \beta$  channels). Thus, a major means by which  $\text{Ca}^{2+}_i$  increases  $P_o$  for both  $\alpha$  and  $\alpha + \beta$  channels is to drive the channels from the gaps between bursts into the bursting states, decreasing the durations of the gaps between bursts.

*The  $\beta$  Subunit Acts Specifically to Stabilize Bursting Activity*

The results in Figs. 1 and 4 A showed that burst duration was markedly greater for  $\alpha + \beta$  channels than for  $\alpha$  channels for data obtained at the same  $\text{Ca}^{2+}_i$ . The results also showed that increasing  $P_o$  by increasing  $\text{Ca}^{2+}_i$  increased burst duration for both  $\alpha$  and  $\alpha + \beta$  channels. Since the  $\beta$  subunit increases  $P_o$  (Fig. 2 A), the greater burst duration for  $\alpha + \beta$  channels could have been a consequence of the increased  $P_o$ , rather than a specific effect of the  $\beta$  subunit on lengthening the bursts.

To distinguish between these two possibilities, the effects of the  $\beta$  subunit on the bursting kinetics were studied at the same  $P_o$  for  $\alpha$  and  $\alpha + \beta$  channels over a wide range of  $P_o$ , obtained by changing  $\text{Ca}^{2+}_i$ . The re-

sults are shown in Fig. 6, where the parameters describing bursting kinetics are plotted against  $P_o$ . When  $\alpha$  and  $\alpha + \beta$  channels were compared at the same  $P_o$  (the  $\text{Ca}^{2+}_i$  was higher for the  $\alpha$  channels to obtain the same  $P_o$ ), mean burst duration was still greatly increased for  $\alpha + \beta$  channels when compared with  $\alpha$  channels (Fig. 6 A), due mainly to increases in both mean open times (Fig. 6 C) and the mean number of openings per burst (Fig. 6 D). Thus, the  $\beta$  subunit directly facilitates bursting, as its effects on bursts are greater than if the  $P_o$  were elevated to the same level in the absence of the  $\beta$  subunit by increasing  $\text{Ca}^{2+}_i$ .

In contrast to the  $\beta$  subunit-induced increases in the burst parameters, the mean durations of the gaps (closed intervals) between bursts were about an order of magnitude less for  $\alpha$  channels than for  $\alpha + \beta$  channels at the same  $P_o$  (Fig. 6 B). Since the  $\beta$  subunit has little effect on the durations of the gaps between bursts (Figs. 4 B and 5), this difference reflects the fact that the data from  $\alpha$  channels were obtained at a higher  $\text{Ca}^{2+}_i$  to obtain the same  $P_o$ . The higher  $\text{Ca}^{2+}_i$  for the  $\alpha$  channels reduced the durations of the gaps between bursts.

*Consistency of Bursting Kinetics as a Function of  $P_o$*

Fig. 7, A and B, plots the mean burst duration and the mean duration of the gaps between bursts against  $P_o$  for five  $\alpha$  and five  $\alpha + \beta$  channels.  $P_o$  ranged from

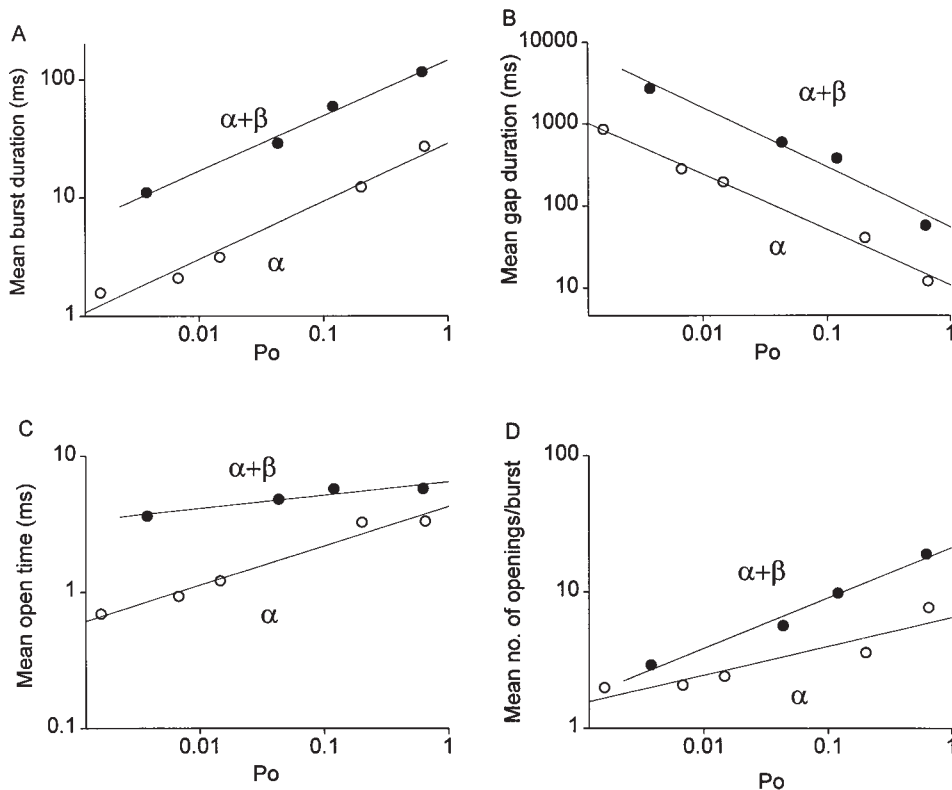


FIGURE 6. Bursting kinetics for  $\alpha + \beta$  channels differ from  $\alpha$  channels at the same  $P_o$ . The indicated bursting parameters are plotted against  $P_o$  for an  $\alpha$  channel and an  $\alpha + \beta$  channel. At any given  $P_o$ , the  $\text{Ca}^{2+}_i$  would be higher for the  $\alpha$  channel than for the  $\alpha + \beta$  channel. The presence of the  $\beta$  subunit led to increases in burst duration (A), mean open time (C), and the number of openings per burst (D), all factors that would increase  $P_o$  for the  $\alpha + \beta$  channels. The decreased durations of the gaps between bursts (B) for  $\alpha$  channels then allowed the two types of channels to have the same  $P_o$ . The  $\alpha$  channel was recorded with symmetrical 175 mM KCl, while the  $\alpha + \beta$  channel was recorded with 175 mM intracellular KCl and 150 mM extracellular KCl. With symmetrical 175 mM KCl, similar findings were obtained for both  $\alpha$  and  $\alpha + \beta$  channels, but over a narrower examined range of  $P_o$ . Effective filtering of 5.1 kHz.  $\alpha$  Channel, C57;  $\alpha + \beta$  channel, C34.

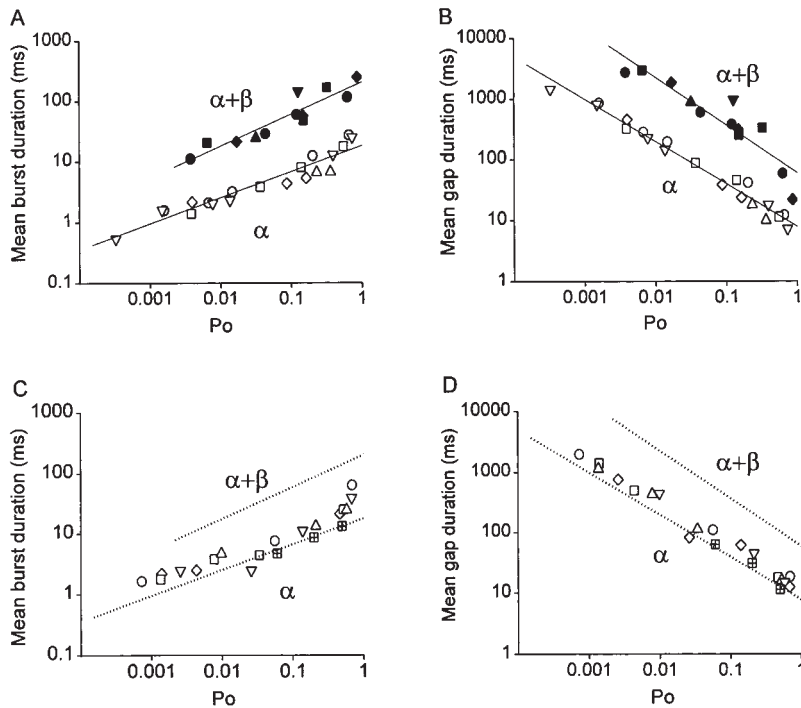


FIGURE 7. Bursting kinetics of native BK channels from cultured rat skeletal muscle suggest that the channels are composed of  $\alpha$  subunits alone. (A and B) The indicated bursting parameters are plotted vs.  $P_o$  for 10 patches, 5 containing a single  $\alpha$  channel (open symbols) and 5 containing a single  $\alpha + \beta$  channel (filled symbols). (C and D) The indicated bursting parameters for six patches, each containing a single native BK channel from cultured rat skeletal muscle, are plotted vs.  $P_o$ . The dotted lines replot the continuous lines from A and B. The bursting kinetics of native BK channels from rat skeletal muscle cluster close to the line for channels composed of  $\alpha$  subunits alone. Each symbol type plots data from a different channel.

$\sim 0.0003$  to  $\sim 0.85$ . The points cluster around the lines (linear least squares fits to the log of the points), indicating a relative lack of variability when these bursting parameters are plotted against  $P_o$ . This can be compared with the data in Fig. 4, E and F, where the variability is greater when the same bursting parameters are plotted against  $Ca^{2+}_i$ . Nevertheless, for both types of plots, the variability among channels of the same type was less than the effect of the  $\beta$  subunit on the indicated bursting parameters.

A variability in the  $Ca^{2+}$  dependence of BK channels has been described previously for native, purified, and cloned channels (Moczydlowski and Latorre, 1983; Singer and Walsh, 1987; McManus and Magleby, 1991; Giangiacomo et al., 1995; Silberberg et al., 1997). Plotting the bursting parameters against  $P_o$  rather than  $Ca^{2+}_i$  may provide a means to remove much of this variability when studying the detailed single-channel kinetics.

#### *Native BK Channels from Cultured Rat Skeletal Muscle Have Bursting Kinetics Like $\alpha$ Channels*

The significant separation of the bursting parameters between  $\alpha$  and  $\alpha + \beta$  channels, together with the relative lack of variability in the parameters for channels of the same type (Fig. 7, A and B), makes it possible to functionally identify whether native BK channels are composed of  $\alpha$  subunits alone, of both  $\alpha$  and  $\beta$  subunits, or of a mixture of the two. Bursting parameters for data from six patches from cultured rat skeletal muscle, each containing a single BK channel, are plot-

ted in Fig. 7, C and D. The dotted lines replot the continuous lines from Fig. 7, A and B, defining the bursting parameters for the cloned  $\alpha$  and  $\alpha + \beta$  channels.

The symbols for the native channels are in the immediate vicinity of the line for the bursting parameters of  $\alpha$  channels. The simplest explanation of these observations is that native BK channels from cultured rat skeletal muscle are composed of  $\alpha$  subunits alone. This conclusion is consistent with the studies of Tseng-Crank et al. (1996) and Chang et al. (1997) who found low or no  $\beta$  mRNA expression in human, canine, or rat skeletal muscle. We cannot exclude, however, that the native channels may have one or more  $\beta$  subunits per channel, but appear to gate like  $\alpha$  channels because of other factors. For example, the alternative splice structure of BK channels can alter gating (Lagrutta et al., 1994). Since the structure of the studied native BK channels is not known, they may be of a different splice variant than the cloned channels.

#### *The $\beta$ Subunit Inhibits Entry into Subconductance States*

Ion channels can enter subconductance levels during gating, reflecting the entry of the channel into conformations that are not fully open or are perhaps partially blocked (Barrett et al., 1982; Chapman et al., 1997; Premkumar et al., 1997; Zheng and Sigworth, 1997). Fig. 8 shows a typical example of gating to a subconductance level that was observed in  $\alpha$  channels, but was seldom observed in  $\alpha + \beta$  channels. To examine the subconductance gating, 210 min of current records from

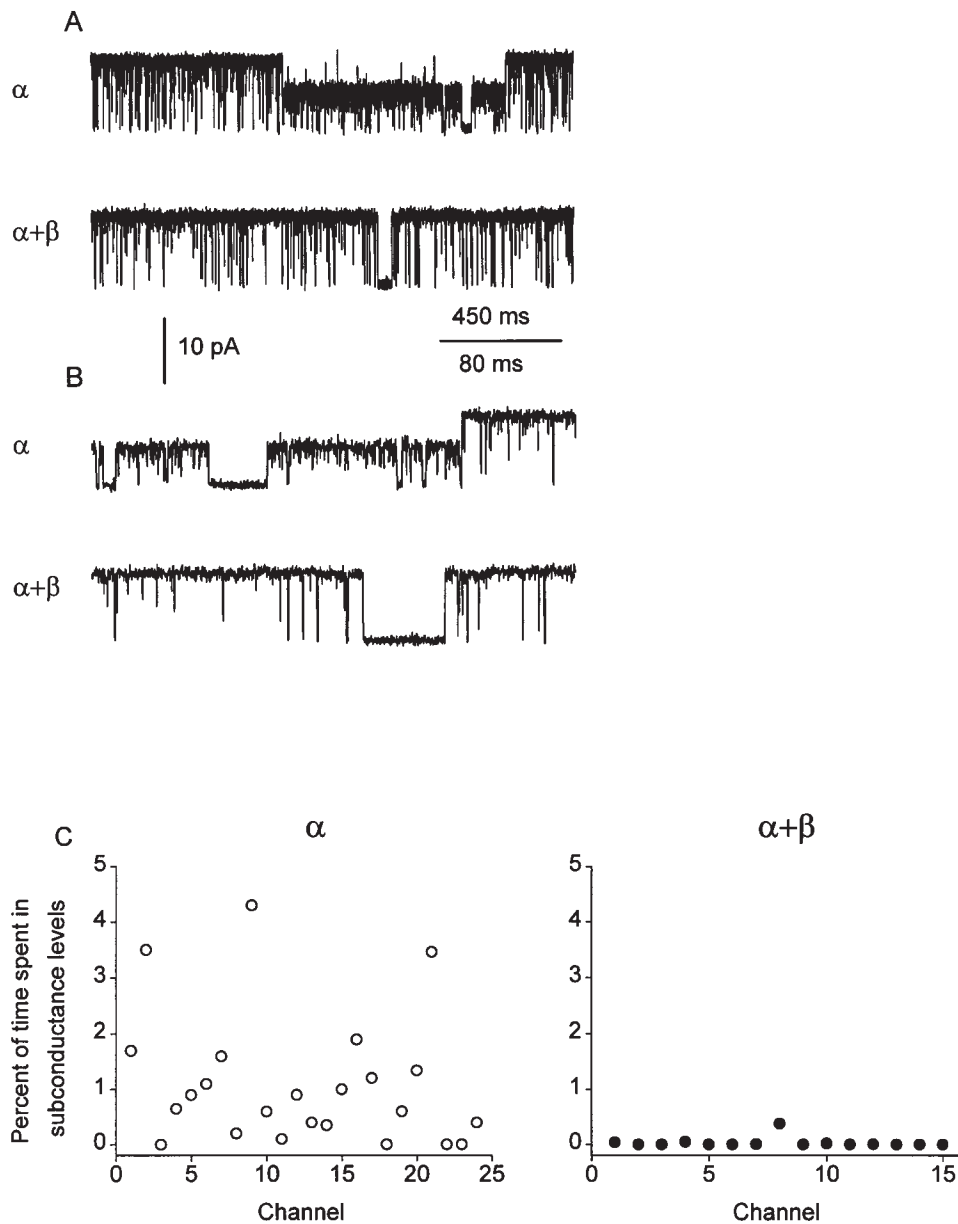


FIGURE 8. The  $\beta$  subunit stabilizes the channel in the fully open conductance level rather than in subconductance levels. Representative single-channel current traces from an  $\alpha$  channel with subconductance gating and from an  $\alpha + \beta$  channel without subconductance gating are presented on a slower time base in A and a faster time base in B. The fully open conductance level for both the  $\alpha$  and  $\alpha + \beta$  channels shown was  $\sim 315$  pS. The subconductance level typically had an amplitude of about half the value of the full conductance level.  $Ca^{2+}_i$  was  $18 \mu M$  for the  $\alpha$  channel and  $5.4 \mu M$  for the  $\alpha + \beta$  channel. Same channels and filtering as used for Fig. 1. (C) Percent time spent in subconductance gating for 24  $\alpha$  channels and 15  $\alpha + \beta$  channels with a  $P_o > 0.7$ . The data were visually screened for transitions to subconductance gating with a duration longer than 50 ms. The membrane potential was  $+30$  mV and the  $Ca^{2+}_i$  ( $3\text{--}100 \mu M$ ) gave a  $P_o$  of  $0.70\text{--}0.96$ . The first 14  $\alpha$  channels and first 9  $\alpha + \beta$  channels were recorded with 175 mM intracellular KCl and 150 mM extracellular KCl, while the next 10  $\alpha$  channels and 6  $\alpha + \beta$  channels were recorded with symmetrical 175 mM KCl.

24  $\alpha$  channels and 230 min from 15  $\alpha + \beta$  channels were visually inspected for transitions to subconductance levels with durations longer than 50 ms. There were 382 transitions to such subconductance levels with a mean duration of 0.4 s for the  $\alpha$  channels, 9 transitions with a mean duration of 0.3 s, and 1 transition with a duration of 9 s for the  $\alpha + \beta$  channels. The total time spent in subconductance levels for each channel was divided by the total time of the recording for that channel and converted to percentage for the plots in Fig. 8 C.

The mean percentage of time that  $\alpha$  channels spent gating to subconductance levels ( $1.1 \pm 1.2\%$ , mean  $\pm$  SD) was decreased 32-fold ( $P < 0.0003$ , Mann-Whitney test) in the  $\alpha + \beta$  channels ( $0.034 \pm 0.097\%$ ). While 20

of 24  $\alpha$  channels spent  $>0.1\%$  of their time gating to subconductance levels, only 1 of 15  $\alpha + \beta$  channels did. Thus, the  $\beta$  subunit inhibits entry into partially conducting states that give subconductance levels of the type shown in Fig. 8.

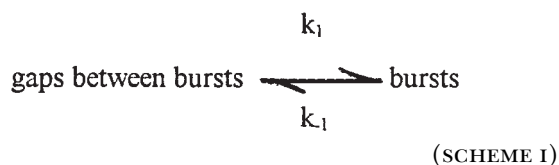
#### DISCUSSION

The accessory  $\beta$  subunit of mammalian BK channels greatly increases  $Ca^{2+}$  sensitivity (McManus et al., 1995; Dworetzky et al., 1996; Meera et al., 1996; Tseng-Crank, et al., 1996). The single-channel analysis in our study provides insight into the mechanism for this apparent increase in  $Ca^{2+}$  sensitivity. We found that the  $\beta$  subunit increased burst duration 20–100-fold by increasing

both the number of openings per burst and the mean open times, while having little effect on the mean durations of the gaps (closed intervals) between bursts.

The bursting kinetics of channels can be described by the highly simplified Scheme I, where  $k_1$  is the rate constant for entering bursts and  $k_{-1}$  is the rate constant for leaving bursts. For simple models that describe the basic single-channel properties of the gating of BK channels, the gaps between bursts in Scheme I are generated by potential transitions among three to eight closed states, and the bursts in Scheme I are generated by potential transitions among three to four open states and three to six brief closed states (Magleby and Pallotta, 1983; McManus and Magleby, 1991; Wu et al., 1995; Rothberg and Magleby, 1998). Because the data in our study were recorded from patches containing a single BK channel, each gap between bursts represents the sum of the dwell times in the closed states entered between bursts for that single channel. Some of the closed states contributing to the gaps between bursts would be expected to bind  $\text{Ca}^{2+}$ , with the binding driving the channel through one or more closed states towards the first open state that terminates the gap between bursts. It is this  $\text{Ca}^{2+}$  dependence of the closed states entered between bursts that produces long gaps between bursts at low  $\text{Ca}^{2+}$  and brief gaps at high  $\text{Ca}^{2+}$ .

Inspection of Scheme I suggests that the  $\beta$  subunit could promote bursting by facilitating the entry of the channel into bursts (by increasing  $k_1$ ) or by preventing the channel from leaving the bursts once entered (by decreasing  $k_{-1}$ ), or by both actions. If the  $\beta$  subunit acts to facilitate entry into bursts, then the durations of the gaps (closed intervals) between bursts should be decreased by the  $\beta$  subunit. Alternatively, if the  $\beta$  subunit acts by retaining the channel in bursts once entered, then the  $\beta$  subunit should have little effect on the durations of the gaps between bursts, but should decrease their relative numbers since the channel would enter the gaps between bursts less often.



Our observations that the  $\beta$  subunit increased burst duration and decreased the numbers of gaps between bursts (Figs. 1, 4 A, and 5) while having little effect on the durations of the gaps between bursts (Figs. 4 B and 5) suggest that the  $\beta$  subunit had little effect on  $k_1$ . Thus, the  $\beta$  subunit increases  $P_o$  mainly by slowing  $k_{-1}$  to retain the channel in the bursting states.

In contrast to the relative lack of effect of the  $\beta$  subunit on the durations of the gaps between bursts, in-

creasing  $\text{Ca}^{2+}_i$  decreased the durations of gaps between bursts for both  $\alpha$  and  $\alpha + \beta$  channels (Figs. 1, 4 B, and 5). Thus, a major means by which  $\text{Ca}^{2+}_i$  increased  $P_o$  for both  $\alpha$  and  $\alpha + \beta$  channels was to increase  $k_1$  to drive the channels from the gaps between bursts into the bursting states. Increasing  $\text{Ca}^{2+}_i$  also increased the durations of the bursts, but not as much as the increase induced by the  $\beta$  subunit for the same increase in  $P_o$  (Figs. 1, 4, and 6).

How might the  $\beta$  subunit effectively slow  $k_{-1}$  to retain the channel in the bursting states? One possibility would be for the  $\beta$  subunit to add additional states that are entered during the bursting. Gating in these additional states could then retain the channel in the bursts. Another possibility would be for the  $\beta$  subunit to add additional  $\text{Ca}^{2+}$  binding sites that would act to retain the channel in bursts. Our observations that the  $\beta$  subunit did not change the numbers of exponential components in the dwell-time distributions (Fig. 3) or the Hill coefficients (Fig. 2) suggest that the  $\beta$  subunit does not act by changing either the numbers of kinetic states entered during gating or the effective number of  $\text{Ca}^{2+}$  binding sites. (Our observations that the number of subunits per channel could be doubled, from four for  $\alpha$  channels to eight for  $\alpha + \beta$  channels, without changing the numbers of detected kinetic states, indicate that the number of states entered during gating is not necessarily related to the total number of subunits comprising the  $\alpha$  channel.)

The above findings, when coupled with previous observations that the  $\beta$  subunit does not appear to change the effective gating charge (McManus et al., 1995; Meera et al., 1996), suggest that the  $\beta$  subunit acts not by fundamental changes in the gating mechanism, such as alterations in either the number of  $\text{Ca}^{2+}$ -binding sites or the number of major conformational changes, but rather through modulation of the gating of the  $\alpha$  subunits.

One possible way the  $\beta$  subunit might modulate the gating of the  $\alpha$  subunits would be through changes in the  $\text{Ca}^{2+}$  binding rates. If the  $\beta$  subunit increased all the  $\text{Ca}^{2+}$ -binding rates to the  $\alpha$  subunits proportionally, then increasing  $\text{Ca}^{2+}_i$  sufficiently to obtain the same  $P_o$  for  $\alpha$  channels as for  $\alpha + \beta$  channels should give the same single-channel kinetics for both types of channels. This was found not to be the case, as the durations of the bursts, the mean open times, the mean numbers of openings per burst, and the durations of the gaps between bursts were all considerably less for  $\alpha$  channels than for  $\alpha + \beta$  channels at the same  $P_o$  (Figs. 5 and 6).

Since the  $\beta$  subunit does not increase all of the  $\text{Ca}^{2+}$ -binding rates proportionally, could it act by increasing a subset of the  $\text{Ca}^{2+}$ -binding rates? Our observation that the  $\beta$  subunit had little effect on the durations of the gaps between bursts suggests that the  $\beta$  subunit has

little effect on the  $\text{Ca}^{2+}$ -binding rates to the closed states that dominate the gaps between bursts. This observation does not exclude the possibility that the  $\beta$  subunit may increase some of the  $\text{Ca}^{2+}$ -binding rates in the bursting states, but such an effect would require a differential effect of the  $\beta$  subunit on the bindings of successive  $\text{Ca}^{2+}$ .

If the  $\beta$  subunit does act by retaining the channel in the bursting states, then this is functionally equivalent to imposing a barrier to prevent the channel from leaving the bursting states. If this is the case, then the deactivation from the bursting states that occurs in the presence of  $\text{Ca}^{2+}$  after a step to negative membrane potentials might be expected to be slowed by the  $\beta$  subunit. Consistent with this possibility, the  $\beta$  subunit does slow deactivation after steps to negative membrane potentials (Dworetzky et al., 1996; Meera et al., 1996; Tseng-Crank et al., 1996).

The  $\beta$  subunit of the BK channel bears no sequence homology with accessory subunits from other channels (Knaus et al., 1994), suggesting that modulatory subunits may have evolved separately as needed to modulate specific channels. It also appears that the  $\beta$  subunit of the BK channel works differently from the modulatory subunits of other channels that increase expression levels and speed activation and inactivation rates (Lacerda et al., 1991; Varadi et al., 1991; Isom et al., 1992; Rettig et al., 1994; Makita et al., 1994; Heinemann et al., 1995; Morales et al., 1995; Shi et al., 1996). However, the actions of the  $\beta$  subunit for the BK channel seem to have some features in common with the actions of the accessory  $\text{Ca}^{2+}$  channel  $\beta_{2A}$  subunit on  $\text{Ca}^{2+}$  channels in the presence of a dihydropyridine derivative; both subunits increase burst duration, although in the case of the  $\text{Ca}^{2+}$  channel this increase occurs only when the  $\text{Ca}^{2+}$  channel is in a high  $P_o$  mode. Interestingly, these increases in burst duration by the different subunits on different channels occur even though the  $\beta$  subunit of BK channels has two putative transmembrane segments (Knaus et al., 1994), while the  $\beta_{2A}$  subunit of  $\text{Ca}^{2+}$  channels is cytoplasmic (Takahashi et al., 1987).

A comparison of the bursting kinetics of BK channels

from cultured rat skeletal muscle to the bursting kinetics of  $\alpha$  channels and  $\alpha + \beta$  channels indicated that BK channels in cultured rat skeletal muscle have bursting kinetics similar to  $\alpha$  channels (Fig. 7). Thus, BK channels in cultured rat skeletal muscle gate as if they are composed of  $\alpha$  subunits alone. This conclusion is consistent with the studies of Tseng-Crank et al. (1996) and Chang et al. (1997), who found low or no  $\beta$  mRNA expression in human, canine, and rat skeletal muscle. In contrast to skeletal muscle, BK channels in tracheal smooth muscle are composed of  $\alpha + \beta$  subunits, and most BK channels in human coronary artery smooth muscle function as if they are composed of  $\alpha + \beta$  subunits (Tanaka et al., 1997). The  $\beta$  subunit would confer a greater  $\text{Ca}^{2+}$  sensitivity to BK channels in smooth muscle.

Our observation that the  $\beta$  subunit of BK channels decreases the percentage of time spent in gating to subconductance levels (Fig. 8) suggests that the  $\beta$  subunit of BK channels stabilizes the full conductance level of the open states. Similar to our observation for BK channels, the presence of an auxiliary subunit for the ryanodine receptor also decreases the percentage of time spent in gating to subconductance levels (Ondrias et al., 1996).

### Conclusion

From a functional viewpoint, it is the retention of the BK channel in the bursting states by the  $\beta$  subunit that increases the apparent  $\text{Ca}^{2+}$  sensitivity of the channel. In the presence of the  $\beta$  subunit, each burst of openings is greatly amplified in duration through increases in both the numbers of openings per burst and in the mean open times. The physical mechanism by which the  $\beta$  subunit retains the channel in the bursting states is not known, but one possibility is that selective allosteric effects of the  $\beta$  subunits on the  $\alpha$  subunits facilitate some conformational changes and/or inhibit others. This selective facilitation and/or inhibition would work to increase the effective energy barrier for leaving the bursting states, through increases in both mean open time and the numbers of openings per bursts.

---

We thank Merck Research Laboratories for providing the mslo (initially cloned by Pallanck and Ganetzky, 1994) and bovine  $\beta$  clones used for transfection, and S. Sine for providing helpful advice on the HEK 293 cell expression system.

This work was supported in part by grants from the American Heart Association, Florida Affiliate (C.M. Nimigeon), the National Institutes of Health (AR32805 to K.L. Magleby), and the Muscular Dystrophy Association.

*Original version received 15 October 1998 and accepted version received 4 December 1998.*

### REFERENCES

- Adelman, J.P., K.Z. Shen, M.P. Kavanaugh, R.A. Warren, Y.N. Wu, A. Lagrutta, C.T. Bond, and R.A. North. 1992. Calcium-activated potassium channels expressed from cloned complementary DNAs. *Neuron*. 9:209–216.
- Atkinson, N.S., G.A. Robertson, and B. Ganetzky. 1991. A component of calcium-activated potassium channels encoded by the *Drosophila slo* locus. *Science*. 253:551–555.
- Barrett, J.N., K.L. Magleby, and B.S. Pallotta. 1982. Properties of

- single calcium-activated potassium channels in cultured rat muscle. *J. Physiol. (Camb.)*. 331:211–230.
- Butler, A., S. Tsunoda, D.P. McCobb, A. Wei, and L. Salkoff. 1993. *mSlo*, a complex mouse gene encoding “maxi” calcium-activated potassium channels. *Science*. 261:221–224.
- Chang, C.-P., S.I. Dworetzky, J. Wang, and M.E. Goldstein. 1997. Differential expression of the  $\alpha$  and  $\beta$  subunits of the large-conductance calcium-activated potassium channel: implication for channel diversity. *Mol. Brain Res.* 45:33–40.
- Chapman, M.L., H.M. VanDongen, and A.M. VanDongen. 1997. Activation-dependent subconductance levels in the drk1 K channel suggest a subunit basis for ion permeation and gating. *Biophys. J.* 72:708–719.
- Colquhoun, D., and A.G. Hawkes. 1981. On the stochastic properties of single ion channels. *Proc. R. Soc. Lond. B Biol. Sci.* 211:205–235.
- Colquhoun, D., and A.G. Hawkes. 1995. The principles of the stochastic interpretation of ion channel mechanisms. In *Single-Channel Recording*. B. Sakmann and E. Neher, editors. Plenum Publishing Corp., New York. 397–482.
- Colquhoun, D., and F.J. Sigworth. 1995. Fitting and statistical analysis of single-channel records. In *Single-Channel Recording*. B. Sakmann and E. Neher, editors. Plenum Press, New York. 483–587.
- Costantin, J., F. Noceti, N. Qin, X. Wei, L. Birnbaumer, and E. Stefani. 1998. Facilitation by the  $\beta_{2a}$  subunit of pore openings in cardiac  $\text{Ca}^{2+}$  channels. *J. Physiol. (Camb.)*. 507:93–103.
- Cox, D.H., J. Cui, and R.W. Aldrich. 1997. Allosteric gating of a large conductance  $\text{Ca}^{2+}$ -activated  $\text{K}^+$  channel. *J. Gen. Physiol.* 110: 257–281.
- Dworetzky, S.I., C.G. Boissard, J.T. Lum-Ragan, M.C. McKay, D.J. Post-Munson, J.T. Trojnecki, C.P. Chang, and V.K. Gribkoff. 1996. Phenotypic alteration of a human BK (hSlo) channel by hSlo $\beta$  subunit coexpression: changes in blocker sensitivity, activation/relaxation and inactivation kinetics, and protein kinase A modulation. *J. Neurosci.* 16:4543–4550.
- Dworetzky, S.I., J.T. Trojnecki, and V.K. Gribkoff. 1994. Cloning and expression of a human large-conductance calcium-activated potassium channel. *Brain Res. Mol. Brain Res.* 27:189–193.
- Garcia-Calvo, M., H.G. Knaus, O.B. McManus, K.M. Giangiacomo, G.J. Kaczorowski, and M.L. Garcia. 1994. Purification and reconstitution of the high-conductance, calcium-activated potassium channel from tracheal smooth muscle. *J. Biol. Chem.* 269:676–682.
- Giangiacomo, K.M., M. Garcia-Calvo, H.-G. Knaus, T.J. Mullmann, M.L. Garcia, and O. McManus. 1995. Functional reconstitution of the large-conductance, calcium-activated potassium channel purified from bovine aortic smooth muscle. *Biochemistry*. 34: 15849–15862.
- Hamill, O.P., A. Marty, E. Neher, B. Sakmann, and F.J. Sigworth. 1981. Improved patch-clamp techniques for high-resolution current recording from cells and cell-free membrane patches. *Pflügers Arch.* 391:85–100.
- Heinemann, S.H., J. Rettig, F. Wunder, and O. Pongs. 1995. Molecular and functional characterization of a rat brain  $\text{K}_v\beta 3$  potassium channel subunit. *FEBS Lett.* 377:383–389.
- Isom, L.L., K.S. De Jongh, D.E. Patton, B.F. Reber, J. Offord, H. Charbonneau, K. Walsh, A.L. Goldin, and W.A. Catterall. 1992. Primary structure and functional expression of the  $\beta 1$  subunit of the rat brain sodium channel. *Science*. 256:839–842.
- Jan, L.Y., and Y.N. Jan. 1997. Cloned potassium channels from eukaryotes and prokaryotes. *Annu. Rev. Neurosci.* 20:91–123.
- Kaczorowski, G.J., H.G. Knaus, R.J. Leonard, O.B. McManus, and M.L. Garcia. 1996. High-conductance calcium-activated potassium channels; structure, pharmacology, and function. *J. Bioenerg. Biomembr.* 28:255–267.
- Knaus, H.G., K. Folander, M. Garcia-Calvo, M.L. Garcia, G.J. Kaczorowski, M. Smith, and R. Swanson. 1994. Primary sequence and immunological characterization of  $\beta$ -subunit of high conductance  $\text{Ca}^{2+}$ -activated  $\text{K}^+$  channel from smooth muscle. *J. Biol. Chem.* 269:17274–17278.
- Lacerda, A.E., H.S. Kim, P. Ruth, E. Perez-Reyes, V. Flockerzi, F. Hofmann, L. Birnbaumer, and A.M. Brown. 1991. Normalization of current kinetics by interaction between the  $\alpha 1$  and  $\beta$  subunits of the skeletal muscle dihydropyridine-sensitive  $\text{Ca}^{2+}$  channel. *Nature*. 352:527–530.
- Lagrutta, A., K.-Z. Shen, R.A. North, and J.P. Adelman. 1994. Functional differences among alternatively spliced variants of slowpoke, a Drosophila calcium-activated potassium channel. *J. Biol. Chem.* 269:20347–20351.
- Latorre, R., A. Oberhauser, P. Labarca, and O. Alvarez. 1989. Varieties of calcium-activated potassium channels. *Annu. Rev. Physiol.* 51:385–399.
- Magleby, K.L. 1992. Ion channels. Preventing artifacts and reducing errors in single-channel analysis. *Methods Enzymol.* 207:763–791.
- Magleby, K.L., and B.S. Pallotta. 1983. Burst kinetics of single calcium-activated potassium channels in cultured rat muscle. *J. Physiol. (Camb.)*. 344:605–623.
- Makita, N., P.B.J. Bennett, and A.L. George, Jr. 1994. Voltage-gated  $\text{Na}^+$  channel  $\beta 1$  subunit mRNA expressed in adult human skeletal muscle, heart, and brain is encoded by a single gene. *J. Biol. Chem.* 269:7571–7578.
- Martell, A.E., and R.M. Smith. 1993. NIST Standard Reference Database 46. Gaithersburg, MD 20899.
- McManus, O.B. 1991. Calcium-activated potassium channels: regulation by calcium. *J. Bioenerg. Biomembr.* 23:537–560.
- McManus, O.B., A.L. Blatz, and K.L. Magleby. 1987. Sampling, log binning, fitting, and plotting durations of open and shut intervals from single channels and the effects of noise. *Pflügers Arch.* 410:530–553.
- McManus, O.B., L.M. Helms, L. Pallanck, B. Ganetzky, R. Swanson, and R.J. Leonard. 1995. Functional role of the  $\beta$  subunit of high conductance calcium-activated potassium channels. *Neuron*. 14: 645–650.
- McManus, O.B., and K.L. Magleby. 1988. Kinetic states and modes of single large-conductance calcium-activated potassium channels in cultured rat skeletal muscle. *J. Physiol. (Camb.)*. 402:79–120.
- McManus, O.B., and K.L. Magleby. 1989. Kinetic time constants independent of previous single-channel activity suggest Markov gating for a large conductance  $\text{Ca}^{2+}$ -activated  $\text{K}^+$  channel. *J. Gen. Physiol.* 94:1037–1070.
- McManus, O.B., and K.L. Magleby. 1991. Accounting for the  $\text{Ca}^{2+}$ -dependent kinetics of single large-conductance  $\text{Ca}^{2+}$ -activated  $\text{K}^+$  channels in rat skeletal muscle. *J. Physiol. (Camb.)*. 443:739–777.
- Meera, P., M. Wallner, Z. Jiang, and L. Toro. 1996. A calcium switch for the functional coupling between  $\alpha$  (hSlo) and  $\beta$  subunits ( $\text{K}_{\text{V,Ca}}\beta$ ) of maxi K channels. *FEBS Lett.* 382:84–88.
- Meera, P., M. Wallner, M. Song, and L. Toro. 1997. Large conductance voltage- and calcium-dependent  $\text{K}^+$  channel, a distinct member of voltage-dependent ion channels with seven N-terminal transmembrane segments (S0–S6), an extracellular N terminus, and an intracellular (S9–S10) C terminus. *Proc. Natl. Acad. Sci. USA*. 94:14066–14071.
- Moczyldowski, E., and R. Latorre. 1983. Gating kinetics of  $\text{Ca}^{2+}$ -activated  $\text{K}^+$  channels from rat muscle incorporated into planar lipid bilayers: evidence for two voltage-dependent  $\text{Ca}^{2+}$  binding reactions. *J. Gen. Physiol.* 82:511–542.
- Morales, M.J., R.C. Castellino, A.L. Crews, R.L. Rasmusson, and H.C. Strauss. 1995. A novel  $\beta$  subunit increases rate of inactivation of specific voltage-gated potassium channel  $\alpha$  subunits. *J. Biol. Chem.* 270:6272–6277.
- Ondrias, K., A.M. Brillantes, A. Scott, B.E. Ehrlich, and A.R. Marks. 1996. Single channel properties and calcium conductance of the

- cloned expressed ryanodine receptor/calcium-release channel. *Soc. Gen. Physiol. Ser.* 51:29–45.
- Pallanck, L., and B. Ganetzky. 1994. Cloning and characterization of human and mouse homologs of the *Drosophila* calcium-activated potassium channel gene, *slowpoke*. *Hum. Mol. Genet.* 3:1239–1243.
- Premkumar, L.S., F. Qin, and A. Auerbach. 1997. Subconductance states of a mutant NMDA receptor channel kinetics, calcium, and voltage dependence. *J. Gen. Physiol.* 109:181–189.
- Rettig, J., S.H. Heinemann, F. Wunder, C. Lorra, D.N. Parcej, J.O. Dolly, and O. Pongs. 1994. Inactivation properties of voltage-gated K<sup>+</sup> channels altered by presence of  $\beta$ -subunit. *Nature*. 369: 289–294.
- Rothberg, B.S., R.A. Bello, L. Song, and K.L. Magleby. 1996. High Ca<sup>2+</sup> concentrations induce a low activity mode and reveal Ca<sup>2+</sup>-independent long shut intervals in BK channels from rat muscle. *J. Physiol. (Camb.)*. 493:673–689.
- Rothberg, B.S., and K.L. Magleby. 1998. Kinetic structure of large-conductance Ca<sup>2+</sup>-activated K<sup>+</sup> channels suggests that the gating includes transitions through intermediate or secondary states. A mechanism for flickers. *J. Gen. Physiol.* 111:751–780.
- Salkoff, L., K. Baker, A. Butler, M. Covarrubias, M.D. Pak, and A. Wei. 1992. An essential 'set' of K<sup>+</sup> channels conserved in flies, mice and humans. *Trends Neurosci.* 15:161–166.
- Schreiber, M., and L. Salkoff. 1997. A novel calcium-sensing domain in the BK channel. *Biophys. J.* 73:1355–1363.
- Shen, K.Z., A. Lagrutta, N.W. Davies, N.B. Standen, J.P. Adelman, and R.A. North. 1994. Tetraethylammonium block of Slowpoke calcium-activated potassium channels expressed in *Xenopus* oocytes: evidence for tetrameric channel formation. *Pflügers Arch.* 426:440–445.
- Shi, G., K. Nakahira, S. Hammond, K.J. Rhodes, L.E. Schechter, and J.S. Trimmer. 1996.  $\beta$  Subunits promote K<sup>+</sup> channel surface expression through effects early in biosynthesis. *Neuron*. 16:843–852.
- Sigworth, F.J., and S.M. Sine. 1987. Data transformations for improved display and fitting of single-channel dwell time histograms. *Biophys. J.* 52:1047–1054.
- Silberberg, S.D., A. Lagrutta, J.P. Adelman, and K.L. Magleby. 1996. Wanderlust kinetics and variable Ca<sup>2+</sup>-sensitivity of dSlo, a large conductance Ca<sup>2+</sup>-activated K<sup>+</sup> channel, expressed in oocytes. *Biophys. J.* 71:2640–2651.
- Singer, J.J., and J.V. Walsh, Jr. 1987. Characterization of calcium-activated potassium channels in single smooth muscle cells using the patch-clamp technique. *Pflügers Arch.* 408:98–111.
- Smith, G.L., and D.J. Miller. 1985. Potentiometric measurements of stoichiometric and apparent affinity constants of EGTA for protons and divalent ions including calcium. *Biochim. Biophys. Acta.* 839:287–299.
- Snedecor, G.W., and W.G. Cochran. 1989. Statistical Methods. Iowa State University Press, Ames, IA. 142–144.
- Takahashi, M., M.J. Seagar, J.F. Jones, B.F. Reber, and W.A. Catterall. 1987. Subunit structure of dihydropyridine-sensitive calcium channels from skeletal muscle. *Proc. Natl. Acad. Sci. USA.* 84: 5478–5482.
- Tanaka, Y., P. Meera, M. Song, H.G. Knaus, and L. Toro. 1997. Molecular constituents of maxi K<sub>Ca</sub> channels in human coronary smooth muscle: predominant  $\alpha + \beta$  subunit complexes. *J. Physiol. (Camb.)*. 502:545–557.
- Tseng-Crank, J., C.D. Foster, J.D. Krause, R. Mertz, N. Godinot, T.J. DiChiara, and P.H. Reinhart. 1994. Cloning, expression, and distribution of functionally distinct Ca<sup>2+</sup>-activated K<sup>+</sup> channel isoforms from human brain. *Neuron*. 13:1315–1330.
- Tseng-Crank, J., N. Godinot, T.E. Johansen, P.K. Ahring, D. Strobaek, R. Mertz, C.D. Foster, S.P. Olesen, and P.H. Reinhart. 1996. Cloning, expression, and distribution of a Ca<sup>2+</sup>-activated K<sup>+</sup> channel  $\beta$ -subunit from human brain. *Proc. Natl. Acad. Sci. USA.* 93:9200–9205.
- Varadi, G., P. Lory, D. Schultz, M. Varadi, and A. Schwartz. 1991. Acceleration of activation and inactivation by the  $\beta$  subunit of the skeletal muscle calcium channel. *Nature*. 352:159–162.
- Wallner, M., P. Meera, and L. Toro. 1996. Determinant for  $\beta$ -subunit regulation in high-conductance voltage-activated and Ca<sup>2+</sup>-sensitive K<sup>+</sup> channels: an additional transmembrane region at the N terminus. *Proc. Natl. Acad. Sci. USA.* 93:14922–14927.
- Wei, A., C. Solaro, C. Lingle, and L. Salkoff. 1994. Calcium sensitivity of BK-type K<sub>Ca</sub> channels determined by a separable domain. *Neuron*. 13:671–681.
- Wu, Y.C., J.J. Art, M.B. Goodman, and R. Fettiplace. 1995. A kinetic description of the calcium-activated potassium channel and its application to electrical tuning of hair cells. *Prog. Biophys. Mol. Biol.* 63:131–158.
- Zheng, J., and F.J. Sigworth. 1997. Selectivity changes during activation of mutant *Shaker* potassium channels. *J. Gen. Physiol.* 110: 101–117.